# PML clastosomes prevent nuclear accumulation of mutant ataxin-7 and other polyglutamine proteins

Alexandre Janer,[1,2,3] Elodie Martin,[1,2,3] Marie-Paule Muriel,[1,2,3] Morwena Latouche,[1,2,3] Hiroto Fujigasaki,[6] Merle Ruberg,[1,2,3] Alexis Brice,[1,2,3,4] Yvon Trottier,[5] and Annie Sittler[1,2,3]

[1]Institut National de la Santé et de la Recherche Médicale U679, Neurologie et Thérapeutique Expérimentale, 75651 Paris Cedex 13, France
[2]Hôpital de la Pitié-Salpêtrière, 75651 Paris Cedex 13, France
[3]Faculté de Médecine, Université Pierre et Marie Curie, 75651 Paris Cedex 13, France
[4]Département de Génétique, Cytogénétique et Embryologie, Groupe Hospitalier Pitié-Salpêtrière, 75651 Paris Cedex 13, France
[5]Département de Pathologie Moléculaire, Institut de Génétique et Biologie Moléculaire et Cellulaire, Institut National de la Santé et de la Recherche Médicale, Centre National de la Recherche Scientifique, Université Louis Pasteur, BP 10142, Illkirch Cedex, CU de Strasbourg, France
[6]Department of Neurology, Musashino Red Cross Hospital, Tokyo 108-8339, Japan

The pathogenesis of spinocerebellar ataxia type 7 and other neurodegenerative polyglutamine (polyQ) disorders correlates with the aberrant accumulation of toxic polyQ-expanded proteins in the nucleus. Promyelocytic leukemia protein (PML) nuclear bodies are often present in polyQ aggregates, but their relation to pathogenesis is unclear. We show that expression of PML isoform IV leads to the formation of distinct nuclear bodies enriched in components of the ubiquitin-proteasome system. These bodies recruit soluble mutant ataxin-7 and promote its degradation by proteasome-dependent proteolysis, thus preventing the aggregate formation. Inversely, disruption of the endogenous nuclear bodies with cadmium increases the nuclear accumulation and aggregation of mutant ataxin-7, demonstrating their role in ataxin-7 turnover. Interestingly, β-interferon treatment, which induces the expression of endogenous PML IV, prevents the accumulation of transiently expressed mutant ataxin-7 without affecting the level of the endogenous wild-type protein. Therefore, clastosomes represent a potential therapeutic target for preventing polyQ disorders.

## Introduction

Spinocerebellar ataxia 7 (SCA7) is a progressive autosomal dominant neurodegenerative disorder characterized by cerebellar ataxia and visual impairment (David et al., 1997) that is due to moderate to severe neuronal loss in the cerebellum and associated structures (Cancel et al., 2000) and degeneration of cone and rod photoreceptors. The SCA7 gene product, ataxin-7 (ATXN7), is a component of the TBP-free TAF-containing complex (TFTC) and the SPT3/TAF9/GCN5 acetyltransferase complex (STAGA), which are implicated in several steps of transcriptional regulation, such as histone acetylation and recruitment of the preinitiation complex to promoters (Scheel et al., 2003; Helmlinger et al., 2004b).

SCA7 belongs to a group of nine inherited neurodegenerative disorders caused by an unstable CAG repeat expansion in gene coding regions, leading to the elongation of a polyglutamine (polyQ) tract in the respective proteins (Stevanin et al., 2002). PolyQ expansions confer toxic properties on mutant proteins, which accumulate aberrantly in neurons, leading to the formation of insoluble nuclear inclusions (NIs), a hallmark of polyQ diseases.

Analysis of mouse models of polyQ disorders showed that accumulation in neuronal nuclei of proteins with expanded polyQ is an important step in pathogenesis (Yvert et al., 2001; Watase et al., 2002; Goti et al., 2004). In SCA7 transgenic and knockin mouse models, progressive retinal degeneration correlates with nuclear accumulation of mutant ATXN7 and altered transcription of photoreceptor genes (La Spada et al., 2001; Yoo et al., 2003; Helmlinger et al., 2004a). Several mechanisms have been proposed to underlie polyQ toxicity in the nucleus (Michalik and Van Broeckhoven, 2003), including sequestration into NIs of nuclear proteins, such as transcription factors, nuclear body components, constituents of the ubiquitin-proteasome system (UPS) and chaperones, which might impair their functions. In the case of SCA7, it was recently shown that mutant ATXN7 alters the functions of the TFTC and STAGA complexes (McMahon et al., 2005; Palhan et al., 2005; Helmlinger et al., 2006).

Correspondence to Annie Sittler: sittler@ccr.jussieu.fr

Abbreviations used in this paper: FMRP, fragile X mental retardation protein; INF, interferon; NI, nuclear inclusion; PML, promyelocytic leukemia protein; polyQ, polyglutamine; SCA7, spinocerebellar ataxia 7; UPS, ubiquitin-proteasome system.

The online version of this article contains supplemental material.


The Journal of Cell Biology, Vol. 174, No. 1, July 3, 2006 65–76
http://www.jcb.org/cgi/doi/10.1083/jcb.200511045

Accumulation of polyQ-expanded proteins in the nucleus may be due to a defect in protein folding, turnover, or degradation. As neurons are postmitotic and long-lived cells, failure to prevent the accumulation of toxic proteins may compromise their survival. Accordingly, molecules that prevent nuclear accumulation or increase the clearance of misfolded polyQ proteins were protective against polyQ toxicity in mouse models (Sanchez et al., 2003; Tanaka et al., 2004; Waza et al., 2005). An understanding of the mechanisms whereby mutant proteins accumulate, aggregate, or are eliminated in the nucleus would help in the development of therapeutic strategies for these diseases.

Previous studies showed that promyelocytic leukemia protein (PML) nuclear bodies colocalized with polyQ-containing proteins in nuclear matrix preparations of cells expressing ATXN7 or ataxin-1 (Skinner et al., 1997; Kaytor et al., 1999). Furthermore, the normal nuclear distribution of PML was altered by the expression of mutant ataxin-1 and -3 (Skinner et al., 1997; Chai et al., 1999). In the brains of patients with SCA7 or other polyQ disorders, PML bodies often colocalized with neuronal NIs (Takahashi et al., 2003). Interestingly, colocalization of PML bodies occurred more frequently in small than in large NIs (Takahashi et al., 2002), suggesting that PML bodies are associated with early steps of polyQ protein aggregation.

PML bodies are multiprotein complexes distributed in a speckled pattern throughout the nucleus (Jensen et al., 2001; Negorev and Maul, 2001; Borden, 2002), where they have been suggested to play a role in many cellular processes, such as transcriptional regulation, growth control, and apoptosis (Seeler and Dejean, 1999; Zhong et al., 2000). The heterogeneous composition and morphology of PML bodies has led to the suggestion that the different PML isoforms have distinct cellular functions (Beech et al., 2005). Because of the variety of partner proteins found in PML bodies, it has also been proposed that PML bodies might be storage compartments for nuclear proteins (Negorev and Maul, 2001). However, clastosomes, a subset of PML bodies, contain components of the UPS and were suggested to be sites of protein degradation in the nucleus (Lafarga et al., 2002). Clastosomes appear to be transient structures that assemble when proteolysis is highly active in the nucleus but disappear when the proteasome is inhibited (Lafarga et al., 2002). Interestingly, Muratani et al. (2002) showed that some PML bodies move about rapidly in the nucleus in an energy-dependent fashion and suggested that these dynamic PML bodies may be nuclear sensors of foreign or misfolded proteins, including those of viral origin, and would thus act like a subnuclear immune system. This is consistent with the observation that interferon (INF) induces PML expression and stimulates the formation of PML bodies (Regad and Chelbi-Alix, 2001).

In this study, we aimed at understanding the role of PML bodies in the fate of polyQ-expanded ATXN7 in the nucleus. Modifying the level and composition of PML bodies dramatically affects the aggregation of mutant ATXN7. We show that a specific isoform of PML, PML IV, orchestrates the recruitment of components of the UPS, chaperones, and mutant ATXN7 (and other expanded polyQ proteins) in specialized nuclear bodies that resemble clastosomes to promote their degradation. The capacity of the nucleus to degrade proteins can be modulated to prevent the toxic accumulation of expanded polyQ proteins.

## Results

### Aggregated ATXN7 colocalizes with PML bodies in SCA7 transgenic mice

We previously showed that PML bodies colocalized with a subset of polyQ aggregates in the brains of patients with SCA7 (Takahashi et al., 2002). To determine whether this was also the case in models of SCA7, we examined the brains of transgenic mice B7E2.B, which express mutant ATXN7 with 128 glutamines ubiquitously in the central nervous system and develop progressive ataxia (Yvert et al., 2001). Mutant ATXN7 accumulated in most neurons, including the cerebellar Purkinje cells (Fig. 1 a) and retinal neurons (Fig. 1, b–d), leading to NI formation. A subset of large ATXN7 aggregates in Purkinje cells (Fig. 1 a) and retinal ganglion neurons (Fig. 1 b) contained PML bodies. Ganglion neurons also had small ATXN7 aggregates, which were either sparsely distributed in the nucleus or juxtaposed to large aggregates. PML bodies colocalized with

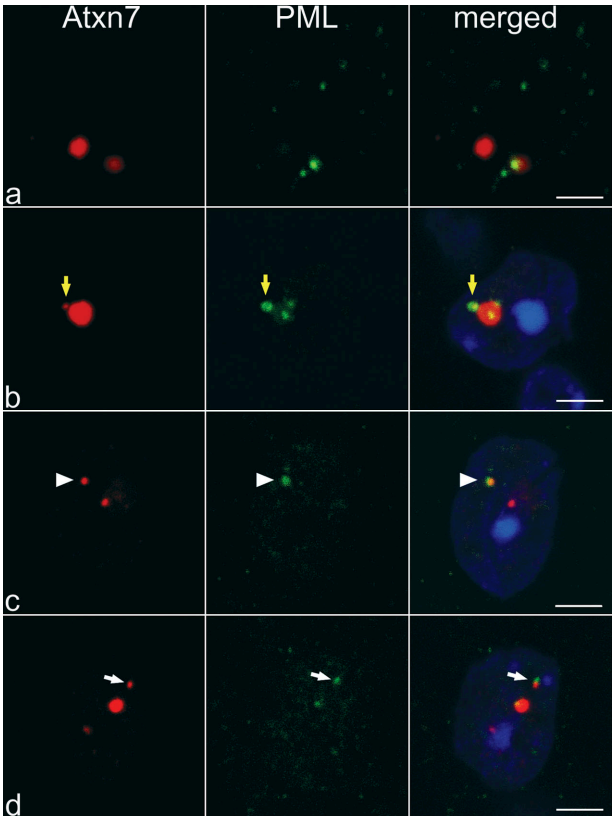


Figure 1. **ATXN7 aggregates colocalize with PML bodies in SCA7 transgenic mice.** Immunofluorescence analysis of cerebellar Purkinje cells (a) and retinal ganglion neurons (b–d) using antibodies against ATXN7 (affinity-purified polyclonal antibody 1261) and PML (chicken anti-PML antibody). Large ATXN7 aggregates sequestered PML bodies (a and b). In ganglion neurons, PML bodies were also surrounded by (b, yellow arrows), colocalized with (c, arrowheads), or juxtaposed to (d, white arrows) small ATXN7 aggregates. The same ganglion neuron on two different focal plans, shown in panels c and d, displayed distinct colocalization between PML bodies and ATXN7 aggregates. Bars, 5 μm.

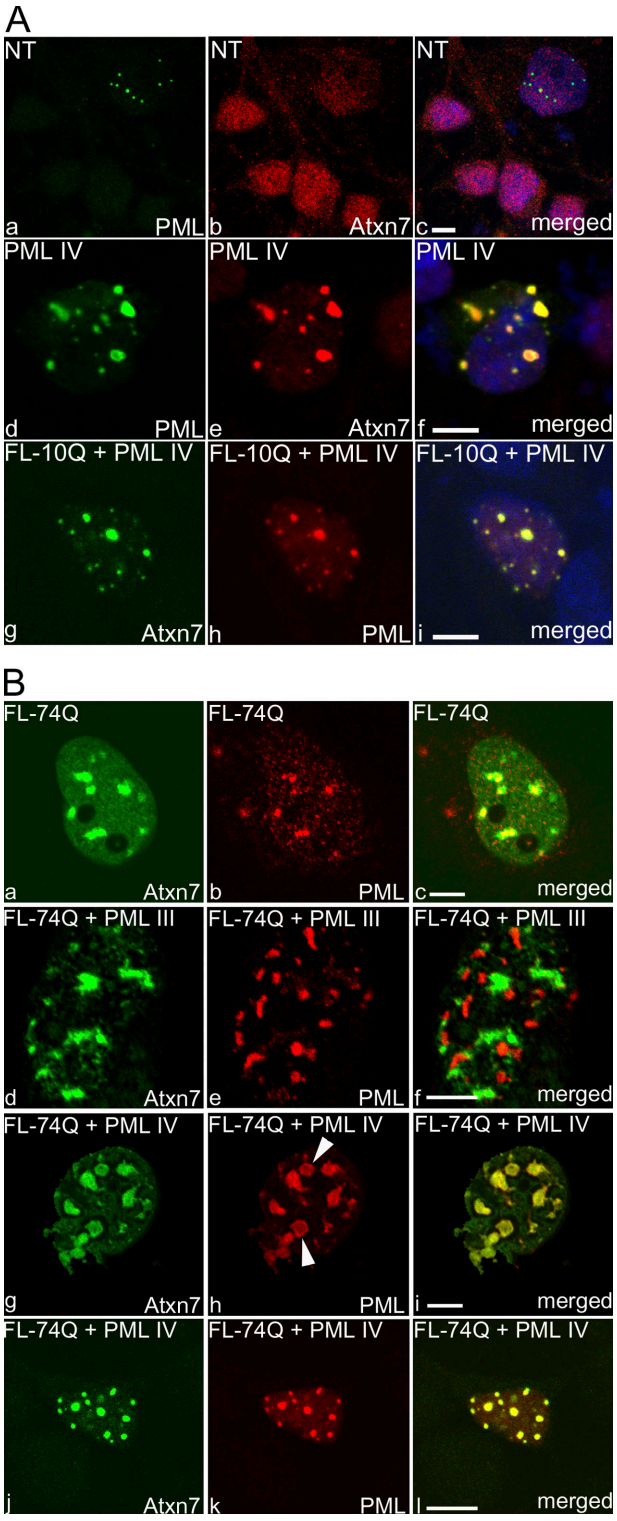


Figure 2. **PML isoform IV relocalizes both endogenous and exogenous wild-type and mutant ATXN7.** (A) In untransfected cortical neurons (NT), endogenous PML (a) did not colocalize with endogenous ATXN7 (b); note that endogenous nuclear bodies, which can be very small, are not detected in all neurons. Overexpressed PML IV relocalized both endogenous ATXN7 (d–f) and overexpressed wild-type ATXN7 (FL-10Q; g–i) to PML IV bodies. (B) In COS-7 cells, full-length mutant ATXN7 (FL-74Q) partially colocalized with endogenous PML bodies (a–c) and did not colocalize with PML III (d–f) but colocalized with PML IV in large round PML bodies (g–i), some with a ring-like pattern (h, arrowheads). In cortical neurons, FL-74Q and PML IV were also colocalized (j–l). Antibodies used were anti–ATXN7 1C1 and polyclonal anti-PML. Confocal images are shown. Bars, 5 μm.

small aggregates, in some cases forming a ring around the aggregate (Fig. 1, b, c, and d). Some PML bodies were juxtaposed to both small and large aggregates (Fig. 1 d). Colocalization of PML bodies with ATXN7 aggregates, notably small ones, is consistent with our previous study of SCA7 brains and raises the question of how PML bodies affect the aggregation of mutant ATXN7.

### ATXN7 colocalizes with PML bodies in cell culture models

To investigate the relationship between PML bodies and mutant ATXN7, we coexpressed full-length wild-type and mutant ATXN7 with isoforms of PML in neurons and in COS-7 cells. There are seven isoforms of PML, resulting from differential splicing, that form nuclear bodies with different morphologies (Bischof et al., 2002; Beech et al., 2005). We have examined the effect of exogenous expression of PML IV, which was previously shown to induce cellular senescence, apoptosis, and regulate p53 activity (Fogal et al., 2000; Bischof et al., 2002) and may thus be related to neuronal dysfunction or death. The effects of PML III were examined to control for specificity.

Endogenous ATXN7 was distributed homogeneously in a granular pattern throughout the nucleus and did not colocalize with the small endogenous nuclear bodies observed in neurons (Fig. 2 A, a–c). When PML IV was overexpressed in transfected neurons, both endogenous ATXN7 (Fig. 2 A, d–f) and full-length wild-type (FL-10Q) exogenous ATXN7 (Fig. 2 A, g–i) colocalized with PML IV in larger nuclear bodies. In COS-7 cells, mutant ATXN7 with 74Q (FL-74Q) was also distributed homogeneously in the nucleoplasm of the majority of transfected cells when expressed alone (unpublished data). In 10–20% of the cells, however, multiple dense nuclear aggregates were seen that contained endogenous PML bodies in their center (Fig. 2 B, a–c), as well as the Daxx protein, a resident PML body protein (not depicted). Exogenous PML III formed rod-shaped bodies and exogenous PML IV larger patchy structures, some of which had a ring-like shape (unpublished data). When PML III was coexpressed with FL-74Q, both rod-shaped PML III bodies and ATXN7 aggregates were observed, but they rarely colocalized (Fig. 2 B, d–f). In contrast, PML IV and mutant ATXN7 colocalized in large, rounder nuclear structures (Fig. 2 B, g–i) that differed from the dense ATXN7 aggregates but resembled the PML IV bodies in that some had a ring-like shape (Fig. 2 B, h, arrowheads). In primary cultures of rat cortical neurons, PML IV also formed round nuclear bodies, but they were smaller and morphologically more homogenous than in COS-7 cells (Fig. 2 A, d–f). When mutant ATXN7 and PML IV were coexpressed in these neurons (Fig. 2 B, j–l), mutant ATXN7 was localized in the PML IV bodies. These data suggest that PML IV bodies recruit both endogenous ATXN7 and exogenous normal and mutant ATNX7.

### PML IV recruits soluble mutant ATXN7 to nuclear bodies

To determine whether PML IV recruits ATXN7 to the nuclear bodies, we performed video-recorded time-lapse experiments

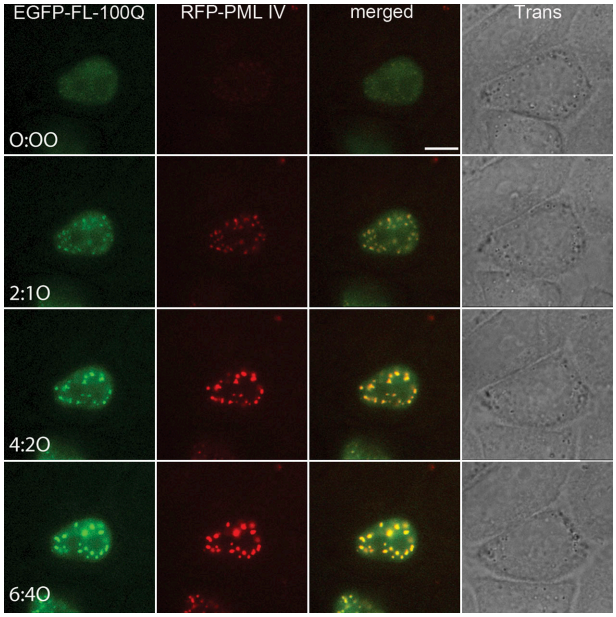


Figure 3. **PML IV rapidly recruits soluble mutant ATXN7 from nucleoplasm to PML IV bodies.** Time-lapse imaging of living HeLa Kyoto cells expressing EGFP-FL-100Q and RFP-PML IV. 6 h after transfection, cells expressing low levels of EGFP-FL-100Q were monitored every 10 min for a period of 16 h. A series of representative images taken during a 6-h, 40-min time period is shown. From the moment PML IV bodies (red) formed (2 h, 10 min), EGFP-FL-100Q (green) relocalized from the nucleoplasm to these tiny red dots. At 4 h, 20 min, small PML IV bodies coalesced into larger bodies and recruited more EGFP-FL-100Q. At 6 h, 40 min, fusion of ATXN7-containing PML IV bodies was more pronounced, preventing ATXN7 accumulation in the nucleoplasm. Bar, 10 μm.

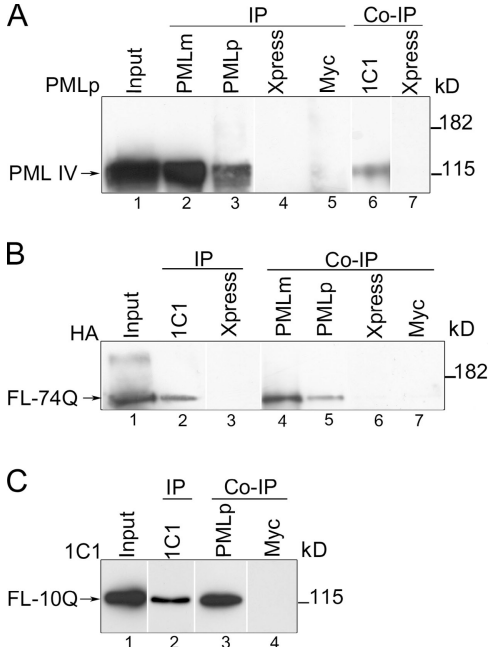


Figure 4. **ATXN7 interacts with PML IV.** (A and B) Mutant (FL-74Q) or wild-type (FL-10Q) ATXN7 and PML IV were coexpressed in COS-7 cells and immunoprecipitated (IP) or coimmunoprecipitated (Co-IP). Antibodies used were as follows: 1C1 monoclonal anti-ATXN7, PML monoclonal (PMLm), PML polyclonal (PMLp), anti-Xpress (monoclonal negative control), and anti-Myc (polyclonal negative control). (A) Immunoprecipitation of PML IV (lanes 2 and 3) and coimmunoprecipitation of PML IV with ATXN7 (lane 6). Coimmunoprecipitation was not seen with control antibodies (lanes 4, 5, and 7). (B) Immunoprecipitation of mutant ATXN7 (FL-74Q; lane 2) and coimmunoprecipitation with PML (lanes 4 and 5). Coimmunoprecipitation was not seen with control antibodies (lanes 3, 6, and 7). (C) Immunoprecipitation of FL-10Q (lane 2) and coimmunoprecipitation with PML IV (lane 3). Coimmunoprecipitation was not seen with the control antibody (lane 4). The lanes shown in each panel were on the same blots; cuts were made to eliminate lanes irrelevant to the demonstration.

on living HeLa Kyoto cells expressing full-length ATXN7 with 100Q fused to EGFP (EGFP-FL-100Q) and PML IV fused to RFP. The cells were monitored from 6 to 22 h after transfection (i.e., for 16 h). Fig. 3 illustrates the development of ATXN7-containing PML bodies over a period of 6 h and 40 min. In cells expressing EGFP-FL-100Q alone, the intensity of the green fluorescence increased over time up to 22 h after transfection but remained homogeneously distributed in the nucleoplasm (unpublished data), indicating that endogenous PML bodies do not form ATXN7-positive bodies. In the presence of RFP-PML IV (red), EGFP-FL-100Q fluorescence remained weak in the nucleoplasm but increased in PML IV bodies from the moment they formed (Fig. 3), indicating that the soluble form of mutant ATXN7 was recruited to the PML IV bodies. Small ATXN7-containing PML IV bodies then moved and coalesced into larger bodies. PML IV, therefore, recruits soluble mutant ATXN7 to nascent PML IV bodies, preventing its accumulation in the nucleus and formation of focal aggregates. Coalescence of small bodies into larger ones was also observed in cells expressing RFP-PML IV alone (unpublished data).

## ATXN7 interacts with PML IV

To determine whether recruitment of ATXN7 to PML IV bodies was due to a physical interaction with PML IV in cell nuclei, we performed coimmunoprecipitation experiments. We first verified that two different anti-PML antibodies (monoclonal and polyclonal) immunoprecipitated PML IV (Fig. 4 A, lanes 2 and 3) and that the anti-ATXN7 monoclonal antibody 1C1 immunoprecipitated FL-10Q (Fig. 4 C, lane 2) and FL-74Q (Fig. 4 B, lane 2). The control antibodies (anti-myc and anti-Xpress) did not immunoprecipitate either protein (Fig. 4, A [lanes 4, 5, and 7] and B [lanes 3, 6, and 7]). When HA-tagged FL-74Q and PML IV were coexpressed and ATXN7 was immunoprecipitated with 1C1, PML IV coprecipitated in the complex (Fig. 4 A, lane 6). When PML IV was immunoprecipitated, HA-tagged FL-74Q coprecipitated in the complex (Fig. 4 B, lanes 4 and 5). FL-10Q and PML IV also coimmunoprecipitated (Fig. 4 C, lane 3). Therefore, not only mutant full-length ATXN7 but also its wild-type counterpart physically interact, directly or indirectly, with PML IV in nuclear bodies.

## PML IV bodies degrade mutant ATXN7 and prevent aggregate formation

We then determined the effect of PML IV on the biochemical properties of mutant ATXN7. When FL-74Q alone was expressed in COS-7 cells, both soluble and aggregated ATXN7 were detected. The soluble form of mutant ATXN7 appeared as a 150-kD protein on Western blots (Fig. 5 A, top).

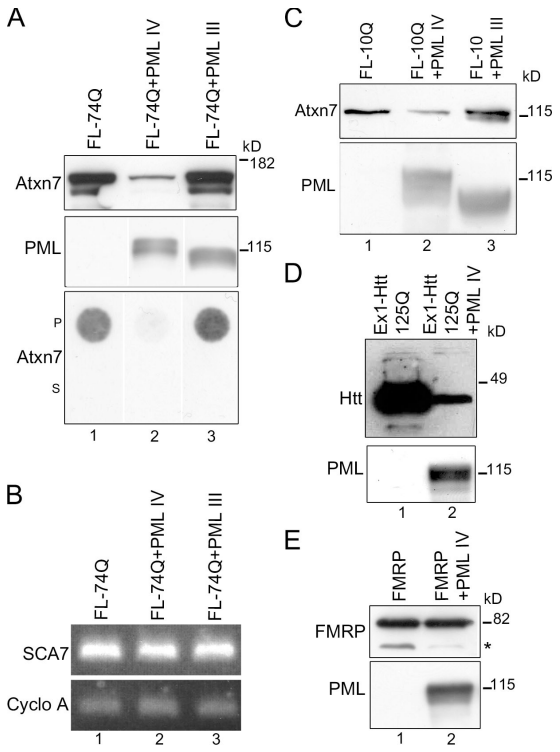


Figure 5. **ATXN7 and Htt-exon1 are efficiently degraded in the presence of PML IV.** (A) Western blot and filter assay of FL-74Q alone or coexpressed with PML IV or III in COS-7 cells. (top) Western blot (30 μg protein, anti–ATXN7 1C1, and anti–PML polyclonal). ATXN7 levels strongly decreased in the presence of PML IV (lane 2) but slightly increased with PML III (lane 3). (bottom) Pellet (P) or supernatant (S) fractions of cell extracts (30 μg protein) were filtered, and SDS-insoluble ATXN7 was revealed by anti–ATXN7 1C1. Coexpression of PML IV led to the disappearance of SDS-insoluble aggregates of mutant ATXN7 (lane 2), whereas PML III slightly increased ATXN7 (lane 3 compared with lane 1). (B) RT-PCR. mRNAs were extracted from cells expressing FL-74Q alone (lane 1) or combined with PML IV (lane 2) or III (lane 3). Primers specific to the SCA7 cDNA and the cyclophilin A (Cyclo A) reference cDNA were used for PCR. Coexpression of PML IV or III had no effect on mutant ATXN7 mRNA. (C) Western blot of cells expressing FL-10Q alone (lane 1) or coexpressed with PML IV (lane 2) or III (lane 3). PML IV decreased and PML III slightly increased ATXN7 levels (same antibodies as in A). (D) Western blot of mutant Htt-exon1 expressed in HeLa cells; Htt-exon1 (Ex1) with 125Q alone (lane 1) or with PML IV (lane 2). Levels of Htt-exon1 (detected with antibody 1C2) were strongly decreased when PML IV was coexpressed. (E) Western blot of FMRP expressed in COS-7 cells alone (lane 1) or with PML IV (lane 2). PML IV did not modify the amount of overexpressed FMRP (detected with antibody 1C3). The asterisk indicates unknown protein degraded in the presence of PML IV. In C, D, and E, the anti-PML antibody was the same as in A.

The aggregated form of the protein was retained on cellulose acetate filters in the filter retardation assay (Fig. 5 A, bottom), which evaluates the overall amount of SDS-insoluble amyloid fibers formed by the aggregation of proteins with expanded polyQ (Wanker et al., 1999). Aggregated ATXN7 was found in the pellet when cell homogenates were centrifuged but not in the supernatant. Coexpression with PML III very slightly increased the amounts of soluble and aggregated ATXN7 (Fig. 5 A, top and bottom). In contrast, coexpression with PML IV led to a strong decrease in the amounts of soluble and aggregated ATXN7 (Fig. 5 A, top and bottom). The supernatant obtained after centrifugation of cell homogenates was also devoid of SDS-insoluble ATXN7. The difference between the effects of PML III and IV was not due to different levels of expression of the isoforms (Fig. 5 A, top) or to differential effects on the transcription of the ATXN7 gene (Fig. 5 B). This suggests that PML IV bodies act directly on the ATXN7 protein by increasing its degradation.

We then examined whether PML IV–dependent degradation of ATXN7 depends on the length of the polyQ tract. When expressed with PML IV, the level of wild-type FL-10Q also decreased (Fig. 5 C), whereas its level slightly increased when expressed in the presence of PML III. Degradation therefore does not depend on the presence of an expanded polyQ tract.

To determine whether PML IV bodies also degrade other polyQ-containing proteins, we coexpressed PML IV with huntingtin (Htt)-exon1 harboring 125Q. PML IV strongly reduced the level of soluble mutant Htt-exon1 (Fig. 5 D). We also verified whether PML IV would degrade an unrelated nuclear protein, fragile X mental retardation protein (FMRP; Sittler et al., 1996) without a polyQ sequence. The level of expression of exogenous FMRP was unaffected by coexpression with PML IV (Fig. 5 E). Intriguingly, a second faint band of lower molecular mass appeared to be decreased by PML IV. Its identity is unknown.

These results show that PML IV bodies recruit both exogenous mutant and normal polyQ-containing proteins and prevent their accumulation in the nucleus but have no effect on another exogenous nuclear protein, FMRP, showing that PML IV targets were not degraded because they were mutated or overexpressed. The targets of PML IV are therefore selective, although the basis for the selectivity is not known.

### PML IV promotes the degradation of mutant ATXN7 by proteasomes

To determine whether PML IV increased the rate of degradation of mutant ATXN7, we performed pulse-chase experiments in COS-7 cells in which mutant ATXN7 was expressed either alone or in combination with PML IV. The degradation of mutant ATXN7 expressed alone was relatively slow, in good agreement with a previously published pulse-chase experiment (Yvert et al., 2001). During the first 8 h of the chase period, only 28% of ATXN7 was degraded (Fig. 6 A). In the presence of PML IV, however, 83% of mutant ATXN7 was degraded after 8 h (Fig. 6 A). The difference between the levels of ATXN7 in the presence and in the absence of PML IV was significant at all time points, starting at 2 h, indicating that PML IV bodies accelerate the degradation of mutant ATXN7.

To see whether the degradation of mutant ATXN7 in the presence of PML IV was mediated by proteasomes, COS-7 cells expressing FL-74Q in the presence and in the absence of PML IV were treated with 5 μM of the proteasome inhibitor MG132. Inhibition of the proteasome increased the amount of mutant ATXN7 in the cells coexpressing FL-74Q and PML IV (Fig. 6 B, compare third and fourth lanes). However, because PML IV was already active before MG132 treatment, it was not possible to accumulate ATXN7 to the level observed without PML. MG132 also increased the level of mutant ATXN7 expressed in the absence of PML IV by impeding normal turnover

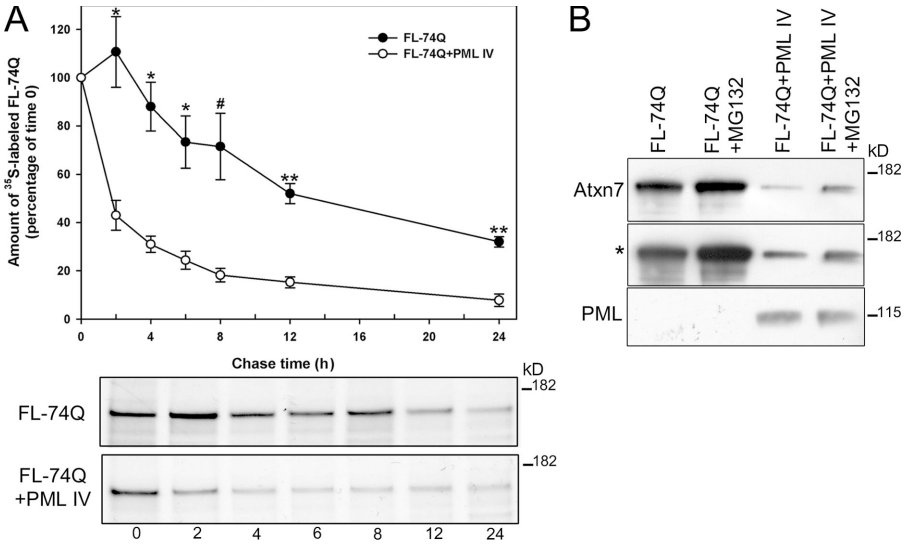


Figure 6. **PML IV promotes the degradation of mutant ATXN7 by proteasomes.** (A) Pulse-chase analysis of the turnover of FL-74Q expressed alone or with PML IV in COS-7 cells. Quantification of immunoprecipitated ATXN7 from four independent experiments are expressed as means ± SEM. *, $P \leq 0.002$; **, $P \leq 0.001$ (paired *t* test). #, $P \leq 0.03$ (Mann-Whitney test). (B) Inhibition of the proteasome by MG132 (5 μM) treatment in COS-7 cells significantly increases the amount of FL-74Q expressed alone (compare first and second lanes) or with PML IV (compare third and fourth lanes). The asterisk indicates longer exposure of the same blot. (bottom) PML IV levels.

of the protein (Fig. 6 B, compare first and second lanes). We thus conclude that the effect of PML IV on the degradation of ATXN7 was mediated by the UPS.

## PML IV bodies recruit UPS components to degrade mutant ATXN7

Under certain stress conditions, PML forms clastosomes that contain components of the UPS (Lafarga et al., 2002). To determine whether PML IV bodies are clastosomes and to understand how they may clear ATXN7, they were analyzed for the presence of UPS components. S10a, a subunit of the 19S non-ATPase regulatory complex of the proteasome was not found in focal aggregates formed by mutant ATXN7 (Fig. 7 A, a–c) but was highly colocalized with PML IV bodies when only PML IV was expressed (Fig. 7 A, d–f). Interestingly, when coexpressed with PML IV, mutant ATXN7 colocalized perfectly

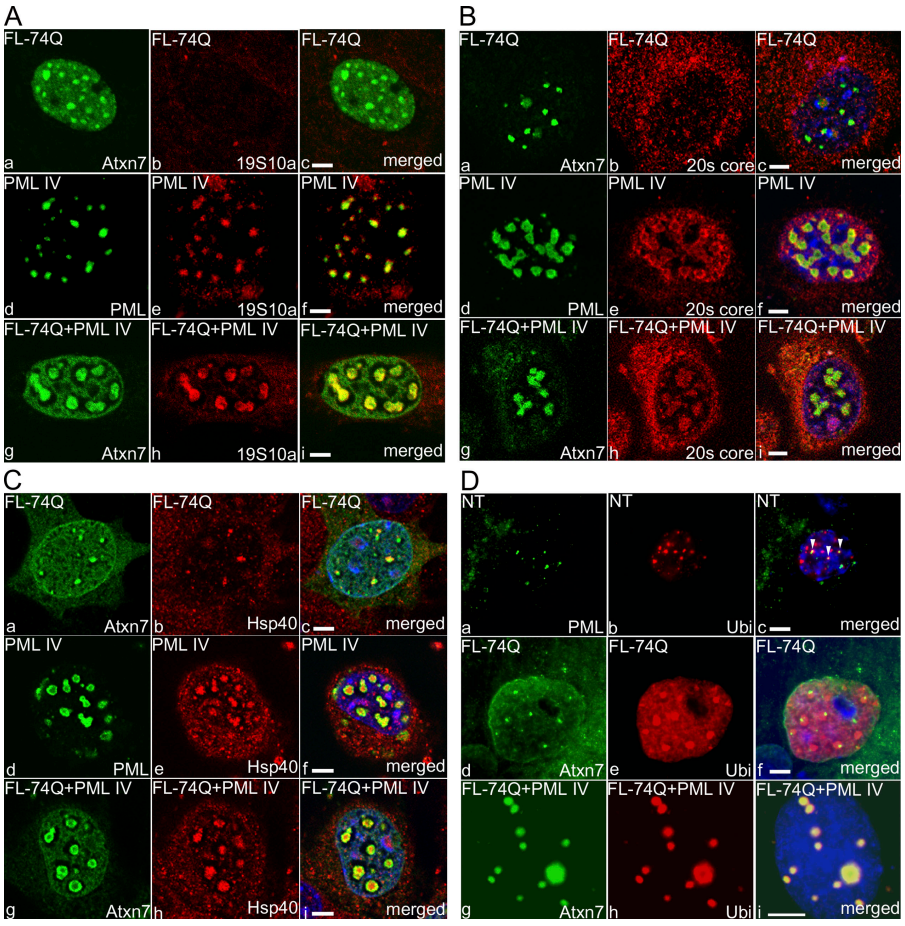


Figure 7. **PML IV bodies recruit UPS components.** (A) S10a, a subunit of the 19S regulatory complex of the proteasome, was not found in focal aggregates formed by mutant ATXN7 (a–c) but was highly colocalized with PML IV bodies when only PML IV was expressed (d–f). When coexpressed with PML IV, mutant ATXN7 colocalized perfectly with the S10a subunit in PML IV bodies (g–i). (B) The 20S catalytic core of the proteasome faintly colocalized with some ATXN7 aggregates (a–c) but strongly colocalized with PML IV expressed alone (d–f) and with ATXN7 present in PML IV bodies (g–i) when both proteins are coexpressed. (C) The Hsp40 chaperone was found in some ATXN7 aggregates (a–c) but to a much greater extent in PML IV bodies (d–f). Hsp40 also strongly colocalized with ATXN7 when it is relocalized in PML IV bodies (g–i). Confocal images are shown. (D) Polyubiquitinylated proteins (labeled with the FK2 antibody) were enriched in PML IV bodies containing ATXN7. Untransfected cells (NT; a–c) contain a subset of endogenous PML bodies (c, arrowheads) that colocalized with polyubiquitinylated proteins. Aggregates of mutant ATXN7 expressed alone (d–f) colocalized faintly with polyubiquitinylated proteins but strongly colocalized with polyubiquitinylated proteins when recruited in PML IV bodies (g–i). Conventional fluorescence was used in D. Bars, 5 μm.

with the S10a subunit in PML IV bodies (Fig. 7 A, g–i). Similar observations were made with two other 19S proteasome subunits, S5a and S6b (Fig. S1, A and B, available at http://www.jcb.org/cgi/content/full/jcb.200511045/DC1); the latter was already detected in endogenous clastosomes (Lafarga et al., 2002). The 20S catalytic core of the proteasome colocalized only with a subset of aggregates in cells expressing FL-74Q alone (Fig. 7 B, a–c), but colocalization was complete with PML IV bodies containing the mutant protein (Fig. 7 B, g–i), as well as with PML IV expressed alone (Fig. 7 B, d–f). This was also observed for subunit α2 of the 20S proteasome (Fig. S1 C). The same was true for the chaperone Hsp40, which recognizes misfolded polyQ proteins (Fig. 7 C). We next verified whether ATXN7 was ubiquitinylated in PML IV bodies. Nontransfected cells possessed only a few PML bodies labeled with an antibody against polyubiquitin that were possibly endogenous clastosomes (Fig. 7 D, a–c, arrowheads indicate colocalization). Aggregates of ATXN7, when expressed alone (Fig. 7 D, d–f), were only slightly labeled with the anti-polyubiquitin antibody, but ATXN7-containing PML IV bodies were strongly labeled (Fig. 7 D, g–i). Together, these data indicate that PML IV induces the assembly of a nuclear structure dedicated to protein degradation, reminiscent of clastosomes. They recruit both chaperones and proteasomes together with its substrates, such as mutant ATXN7, targeted for degradation by polyubiquitin.

### Recruitment of mutant ATXN7 in PML IV bodies prevents polyQ amyloid fiber formation

We investigated the nature of mutant ATXN7 in PML IV bodies by performing an ultrastructural analysis of transfected COS-7 cells. Because truncated mutant ATXN7 aggregates more rapidly than the full-length protein (unpublished data), we expressed Tr-100Q-EGFP (the first 232 amino acids of the protein containing the polyQ stretch fused to EGFP) in the presence or absence of PML IV. We examined ATXN7 distribution by electron microscopy after immunolabeling with a monoclonal anti-ATXN7 antibody and a secondary antibody coupled with 10-nm gold particles. Tr-100Q-EGFP, when expressed alone, was restricted to pale-stained fibrillary structures in the nucleus with fibers radiating from the edges of the aggregates (Fig. 8, A and B). When coexpressed with PML IV, Tr-100Q-EGFP colocalized with PML IV (colabeling with species-specific secondary antibodies coupled with 15-nm gold particles to detect PML) in round or oval structures, which are most likely PML IV bodies (Fig. 8, C and D; arrows [ATXN7] and arrowheads [PML] indicate colocalized gold particles). Importantly, no fibrillary structures were evident in this case (Fig. 8, C and D). This was confirmed by the absence of ATXN7 aggregates on the filter assay (Fig. 8 E). ATXN7 in PML IV bodies was therefore no longer fibrillary in structure and can no longer be considered to be aggregated.

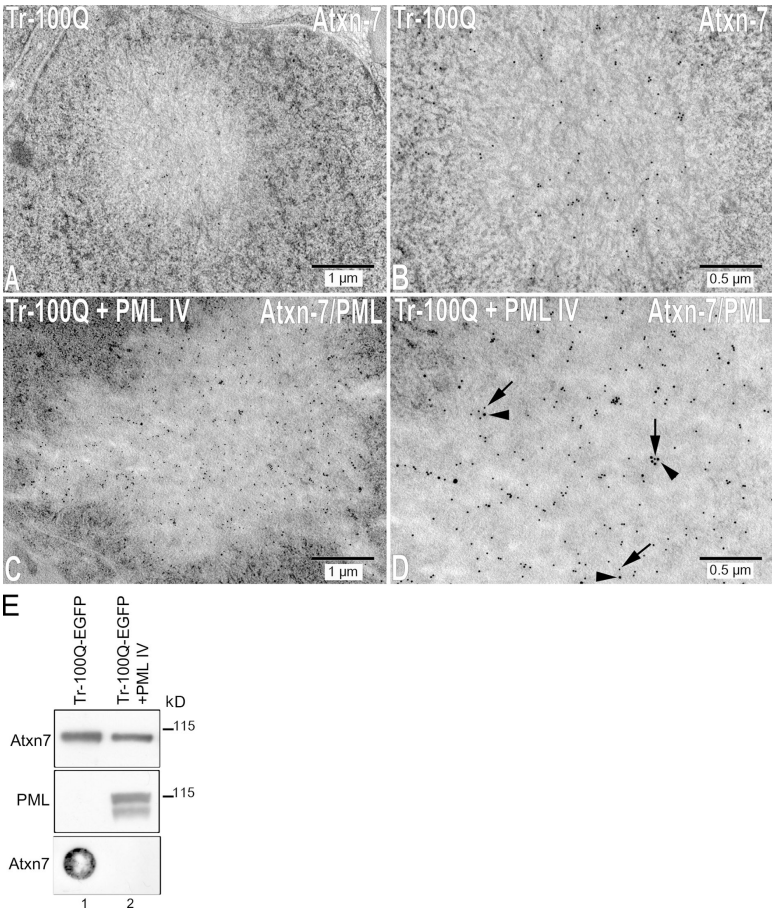


Figure 8. **PML IV prevents the formation of fibrillar structures of mutant truncated ATXN7.** (A–D) Immunoelectron microscopic images of COS-7 cells expressing Tr-100Q-EGFP alone (A and B) or in combination with PML IV (C and D). The following primary antibodies were used: anti–ATXN7 1C1 (mouse) and anti-PML (rabbit). The following secondary antibodies were used: anti-mouse or anti-rabbit immunoglobulins coupled to 10- or 15-nm gold particles, respectively. ATXN7 (10-nm particles) is seen inside an intranuclear inclusion (A) surrounded by long fibers (higher magnification in B). (C and D) When both PML IV and mutant ATXN7 are expressed, colocalization is observed between ATXN7 (10-nm particles, arrows) and PML (15-nm particles, arrowheads). In double-transfected cells, no fibers can be detected. Nuclear membrane is visible in A (top). Bars: (A and C) 1 µm; (B and D) 0.5 µm. (E) Western blot and filter assay of extracts of cells expressing Tr-100Q-EGFP expressed alone or with PML IV. Coexpression of PML IV led to a modest decrease in the level of soluble Tr-100Q (Western blot) but to a strong decrease in the amount of SDS-insoluble Tr-100Q (filter assay).

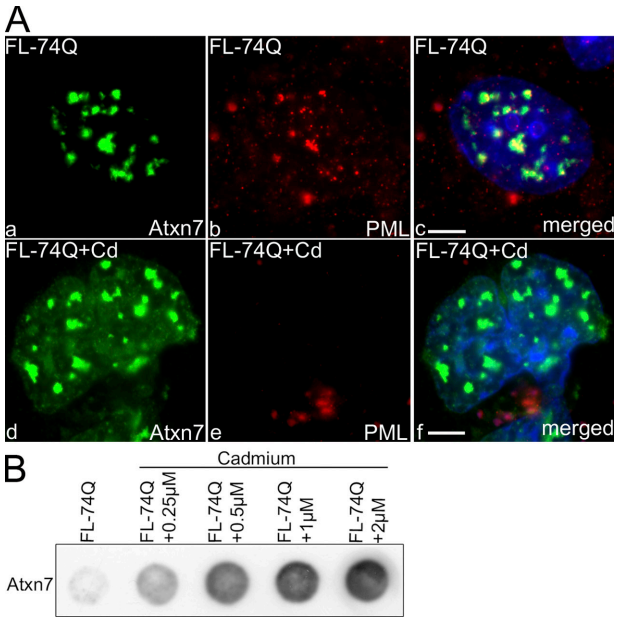


Figure 9. **Cadmium disrupts PML bodies and enhances aggregation of mutant ATXN7.** (A) In untreated COS-7 cells, mutant ATXN7 colocalizes with endogenous PML bodies (a–c). In cells treated with 2 μM cadmium (d–f), PML bodies are disrupted and no longer visible (e). Consequently, large ATXN7 aggregates cannot contain any PML bodies (f). (B) The increase in ATXN7 aggregation is dose dependent in cells treated with 0.25–2 μM cadmium (filter assay on pellet fraction of cell extracts; 50 μg).

Soluble Tr-100Q-EGFP levels analyzed on Western blot were slightly decreased by PML IV expression (Fig. 8 E).

### Cadmium disrupts PML bodies and prevents the degradation of mutant ATXN7 by endogenous clastosomes

To determine whether altering the amount of endogenous PML bodies affects the degradation or aggregation of mutant ATXN7, we treated cells expressing FL-74Q with cadmium chloride, reported to disrupt PML bodies (Nefkens et al., 2003). Immunofluorescence analysis showed that 2 μM cadmium totally disrupted the endogenous PML bodies. Consequently, no colocalization between mutant ATXN7 aggregates and the PML protein was observed (Fig. 9 A, d–f), compared with the untreated cells (Fig. 9 A, a–c). A treatment with increasing concentrations of cadmium (0.25–2 μM) showed that the aggregation of mutant ATXN7 was dose dependent, as shown on filter assay (Fig. 9 B), suggesting that endogenous clastosomes are indeed involved in mutant ATXN7 degradation.

### β-INF stimulates the PML-dependent degradation of mutant ATXN7 and the disappearance of aggregates

Because β-INF was reported to up-regulate the expression of PML (Regad and Chelbi-Alix, 2001), we investigated its effect on the PML-dependent degradation of mutant ATXN7. β-INF increased the size and number of PML bodies in nontransfected COS-7 cells (Fig. 10 A, a and b). Faint endogenous PML immunoreactivity was observed in aggregates of mutant ATXN7 in untreated cells (Fig. 10 A, c–e, arrowheads). β-INF treatment led to the formation of large, strongly immunoreactive PML bodies that colocalized with mutant ATXN7 (Fig. 10 A, f–h). These results also suggest that the presence of mutant ATXN7 promoted the coalescence and fusion of PML bodies into enlarged bodies resembling PML IV bodies, which colocalized perfectly with mutant ATXN7 (Fig. 10 A, compare b and g). Semiquantitative RT-PCR performed with primers that specifically amplify PML IV showed that the expression of PML IV was induced in β-INF–treated cells but not in control cells (Fig. 10 B, lane 2). Western blots show that β-INF increased the levels of several PML isoforms in both untransfected COS-7 cells and cells overexpressing exogenous ATXN7 in its wild-type FL-10Q or mutant form FL-74Q (Fig. 10, C–E). β-INF treatment decreased the amount of overexpressed soluble FL-10Q (Fig. 10 D) and FL-74Q (Fig. 10 E) but had no effect on the level of endogenous wild-type ATXN7 (Fig. 10 C). The PML-dependent degradation of ATXN7 induced by β-INF was mediated by the proteasome, as it was inhibited by MG132 (Fig. 10 F). Interestingly, insoluble mutant ATXN7 disappeared from cells treated with β-INF, as shown by the filter assay, but an insoluble PML-containing material was detected (Fig. 10 G, left, lane 2). This material was independent of ATXN7 expression but dependent on β-INF treatment and attributable to the increased expression of PML IV isoform (Fig. 10 G, right, lanes 2 and 3).

We conclude from these experiments that β-INF induces PML IV expression and increases the presence of clastosomes that degrade ATXN7, preventing its aggregation. The observation that only mutant but not endogenous ATXN7 is degraded in the presence of β-INF suggests that this substance may have therapeutic value.

## Discussion

Accumulation of misfolded polyQ-expansion proteins in neuronal nuclei, ultimately leading to the formation of NIs, is a key step in the pathogenesis of SCA7 and other polyQ-expansion diseases (Michalik and Van Broeckhoven, 2003). We have focused on PML bodies, known to be associated with NIs (Takahashi et al., 2003), which are suggested to be privileged sites of nuclear protein degradation (Lafarga et al., 2002), and have investigated their role in either the degradation or the accumulation of polyQ-containing protein. We report that modifying the level and composition of PML nuclear bodies has profound effects on the fate of disease-causing polyQ-expansion proteins in the nucleus.

Seven PML isoforms have been described that share an $NH_2$-terminal region comprising the RBCC (RING-finger, B-box, coiled-coil domain) but differ in their COOH-terminal region because of alternative splicing (Jensen et al., 2001). The role of each isoform is not yet known, but they might be associated with different functions of the nuclear bodies (Bischof et al., 2002; Muratani et al., 2002; Beech et al., 2005). We have explored the effect of two isoforms, PML III and IV, on the fate of mutant ATXN7 in the nucleus. Although these isoforms differ only by their short COOH-terminal extensions (71 amino acids in PML III and 63 amino acids in PML IV), they form nuclear

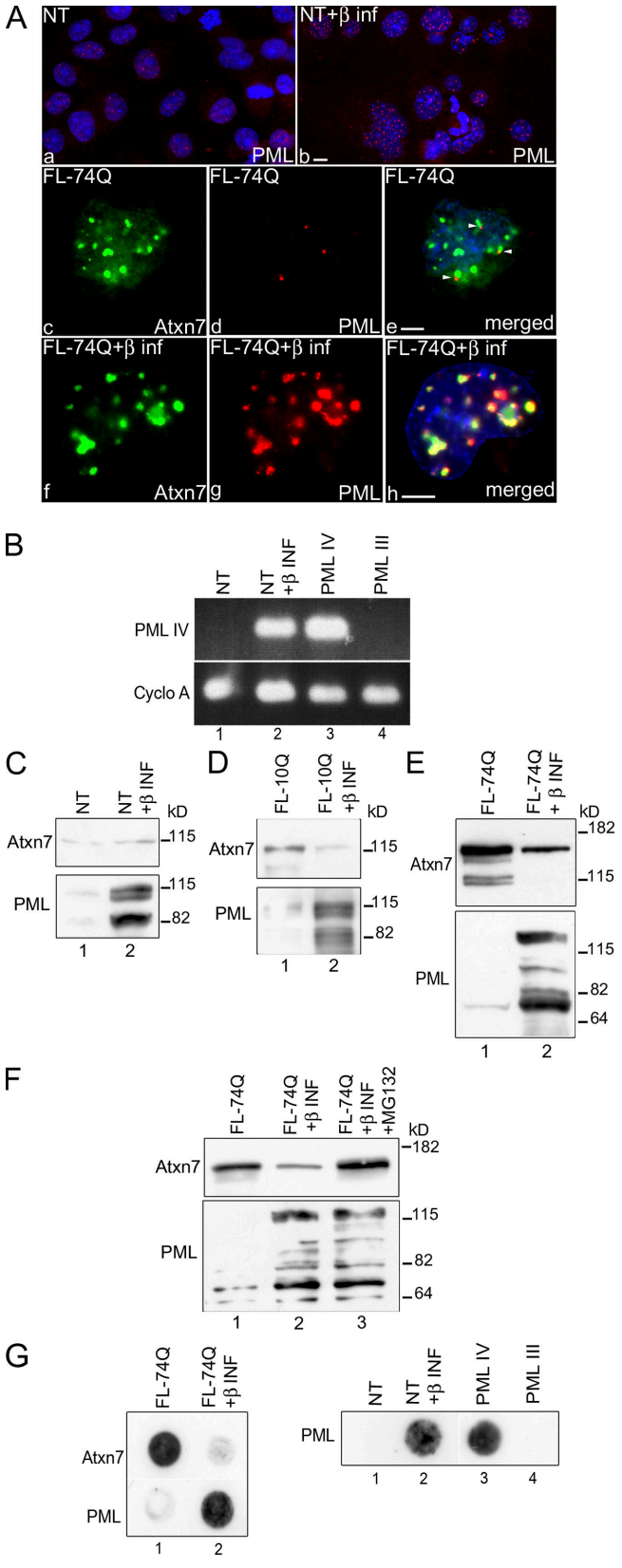


Figure 10. **β-INF treatment leads to the degradation of mutant ATXN7 and the disappearance of aggregates.** (A) β-INF treatment of COS-7 cells, untransfected (a and b) or expressing FL-74Q (c–h). β-INF increases the number and size of PML bodies (red) in untransfected cells (a and b). FL-74Q aggregates colocalized with some endogenous PML bodies (c–e, arrowheads). β-INF treatment increases both the number and size of PML bodies that have strikingly different morphologies and protein composition. PML IV bodies are round and larger than PML III bodies, which are rod shaped. PML IV bodies were highly enriched in proteasome components. They contained subunits of the 19S complex, implicated in unfolding of the substrates, as well as subunits of the 20S catalytic core complex. PML IV bodies also colocalized with the chaperone Hsp40 and polyubiquitinylated proteins and thus resemble clastosomes, a subset of endogenous PML bodies enriched in UPS components, suggested to be sites where nuclear proteins are degraded (Lafarga et al., 2002). Thus, endogenous PML IV appears to be a component of endogenous clastosomes. Whether they also contain other isoforms of PML remains to be determined.

Interestingly, only overexpressed PML IV relocalized endogenous as well as exogenous wild-type and mutant ATXN7 to PML IV bodies. Consequently, because of the presence of UPS components, PML IV actively increased the degradation of the soluble form of mutant ATXN7, which led to the disappearance of SDS-insoluble aggregates. We further demonstrated that the PML IV–dependent degradation of mutant ATXN7 is mediated by the proteasome, showing for the first time that exogenously expressed PML IV clastosomes indeed degrade a substrate, in our case, mutant ATXN7.

Time-lapse experiments showed that PML IV acts on the soluble form of mutant ATXN7 to recruit it to PML IV bodies. Correspondingly, soluble PML IV physically interacts with the soluble forms of mutant and wild-type ATXN7. This suggests that PML IV convoys the soluble forms of ATXN7 to the bodies, where they are degraded by the UPS components, thus preventing the deleterious accumulation of mutant ATXN7. How PML IV selects the substrates for degradation remains to be elucidated. Interestingly, ATXN7 does not interact with PML III (unpublished data) and, consequently, it is not recruited to PML III bodies. However, the immediate early gene X1 (IEX-1), a stress response gene involved in apoptosis, was shown to colocalize with both PML III and IV and to coimmunoprecipitate with PML III but not PML IV (Kruse et al., 2005). These authors noted on Western blots positive coregulation of PML III with IEX-1 but a negative coregulation of PML IV. IEX-1 might therefore be another nuclear substrate for PML IV clastosomes. An investigation of how ATXN7 interacts with PML IV, directly or indirectly, might provide a clue as to how PML IV selects its substrates.

bodies colocalized with mutant ATXN7 (f–h). Conventional fluorescence was used. Bars, 5 μm. (B) RT-PCR with primers specific to PML IV shows that β-INF increases the expression of endogenous PML IV mRNA in nontransfected (NT) cells (compare lanes 1 and 2), the levels of which are compared with overexpressed PML IV (positive control; lane 3) and overexpressed PML III (negative control; lane 4). The reference transcript cyclophilin A (Cyclo A) was amplified in parallel. (C–E) β-INF induces the expression of multiple isoforms of PML. β-INF does not affect the level of endogenous ATXN7 (C) but decreases the levels of transfected wild-type (D) and mutant ATXN7 (E). (F) PML-dependent degradation of ATXN7 induced by β-INF is inhibited by MG132, showing that it is mediated by the proteasome. (G, left) Filter assay shows that ATXN7 aggregates disappear in β-INF–treated cells, but an insoluble PML-containing fraction appears (lane 2). (right) Insoluble PML material was observed either when PML IV was expressed (lane 3) or when NT cells were treated with β-INF (lane 2), but not when PML III was expressed (lane 4).

The SDS-insoluble structures formed by PML IV, consistent with the fact that PML can self-interact and oligomerize (Kastner et al., 1992; Grignani et al., 1996; Jensen et al., 2001), might serve as a scaffold to bring together both the actors of the UPS and the substrates to be degraded. When the level of PML IV is increased by exogenous expression, the composition of the PML bodies changes, leading to the formation of enlarged clastosomes. This increases the capacity of the nucleus to degrade specific substrates, such as toxic polyQ protein. Others have shown that proteasome-dependent protein degradation occurs in nucleoplasmic foci that partially overlap or juxtapose with splicing speckles and PML bodies (Rockel et al., 2005). In a very recent study, a novel GTPase CRAG (CRAM-associated GTPase) induced, under cellular stress, an interaction with PML that formed the enlarged ring structures typical of PML bodies (Qin et al., 2006). Interestingly, it was shown that polyQ accumulation and oxydative stress triggered association of CRAG and polyQ in the cytoplasm before translocation to the nucleus. Once inside the nucleus, CRAG promoted the degradation of polyQ in PML bodies. It would be interesting to know whether CRAG was also implicated in the formation of PML IV bodies in our cell culture model, or whether activation of CRAG by experimental stress can convert endogenous PML bodies that do not degrade ATXN7 to degradation-competent bodies, in the absence of overexpression or β-INF treatment.

Our study with cadmium showed, for the first time, that some endogenous PML bodies, presumably endogenous clastosomes, actively participate in the degradation of mutant ATXN7 and, when disrupted, increase the amount of ATXN7 in cells. The slight increase in the amount of ATXN7 observed when PML III was overexpressed might also explain the disorganization of endogenous clastosomes or a change in their composition. These observations also suggest that endogenous clastosomes are not sufficiently active to prevent the aggregation of mutant ATXN7. The inhibitory effects on aggregation of increased PML IV expression raises the question of whether this would provide the basis of an interesting therapeutic strategy to treat SCA7 or other polyQ disorders.

In the brains of patients, endogenous clastosomes might prevent the accumulation of mutant proteins for several decades before onset of aggregation. Later in the pathogenic process, the balance between clastosome activity and the level of accumulating polyQ proteins might be altered as a result of the disease process or a decrease in proteasome or chaperone activity during aging (Grune et al., 2004; Proctor et al., 2005), leading to the formation of polyQ aggregates. Because the mutant proteins are concentrated in the clastosomes, this might even be a site where the aggregation of proteolytic fragments of the proteins begins. The colocalization of PML bodies and small polyQ aggregates in the brain of patients and animal models supports this hypothesis.

β-INF increased the number and size of PML bodies and decreased the levels of both soluble and aggregated mutant ATXN7. Although the debate concerning the relative contributions of soluble and aggregated polyQ proteins to cellular toxicity has not yet been resolved (Michalik and Van Broeckhoven, 2003), the reduction of either form of the protein could be beneficial to cells. The observation that only mutant but not endogenous ATXN7 is degraded in the presence of β-INF, which is an approved drug used in the treatment of multiple sclerosis (Javed and Reder, 2006), reinforces the hypothesis that this substance may have therapeutic value, as it would not eliminate functional ATXN7. However, it affected the aggregation of mutant ATXN7 in cell cultures only when treatment began before or shortly after transfection with the ATXN7 constructs. This is consistent with the action of PML IV on the soluble form of mutant ATXN7 but not on preexisting aggregates, raising the question of when in the course of SCA7 or other polyQ diseases an effective therapy might be initiated. This should be explored in animal models.

In conclusion, our study shows that the capacity of the nucleus to degrade specific protein substrates is intimately linked to the level and composition of PML bodies. In addition to providing a molecular basis for the accumulation of certain mutant proteins in the nucleus, these findings also suggest that protein degradation through clastosomes can be potentiated to prevent the nuclear accumulation of undesirable proteins, such as those with expanded polyQ, raising the hopes that this mechanism will be adapted to therapeutic ends.

## Materials and methods

### Plasmids

The SCA7 constructs were previously described (Zander et al., 2001). FL-10Q and -74Q, cloned in pCDNA3, contain the full-length wild-type or expanded ATXN7 cDNA, respectively, with FLAG tags at the COOH terminus. FL-74Q contains, in addition, an HA tag at the $NH_2$ terminus. Full-length and truncated ATXN7 containing 100Q were cloned in the pEGFP-N1 vector. A PML IV construct in the pTL2 vector was provided by P. Kastner (Institut de Génétique et de Biologie Moléculaire et Cellulaire, Strasbourg, France). PML IV was amplified by PCR (see the supplemental text, available at http://www.jcb.org/cgi/content/full/jcb.200511045/DC1, for primer sequences) and cloned in pCDNA3. HcRFP-PML IV plasmid was generated by subcloning PML IV from pCDNA3 into pHcRed1-C1 vector (CLONTECH Laboratories, Inc.). All PML constructions were verified by sequencing. The PML III construct in the pSG5 vector was given by A. Dejean (Institut National de la Santé et de la Recherche Médicale, Paris, France).

### RNA preparation and semiquantitative RT-PCR

RNA was extracted from whole-cell lysates of transfected or untransfected COS-7 cells, using the RNAeasy kit (QIAGEN), and cDNAs were synthesized (ThermoScript RT-PCR System; Invitrogen) according to the manufacturer's instructions. PCR was performed using primers specific for the genes of interest. PCR primers for amplification of the SCA7 gene and for the PML IV–specific 3′ end are given in the supplemental text. The cyclophilin A gene was used as the reference.

### Cell culture, transfections, MG132, INF, and cadmium treatments

COS-7 cells were maintained in DME (Invitrogen) supplemented with 5% FBS and 100 IU/ml penicillin plus 100 μg/ml streptomycin. Cell lines were transfected with Lipofectamine-PLUS reagents (Invitrogen) as prescribed. Unless otherwise specified, cells were harvested or analyzed by immunofluorescence 40–45 h after transfection. 2,000 IU/ml β-INF (Sigma-Aldrich) was added to the culture medium after plating and during transfection. Cadmium chloride (0.25–2 μM) was added during transfection. For proteasome inhibition, 5 μM MG132 was applied for 12 h at 25 h after transfection.

Cultures of postmitotic neurons were prepared from the cortex of embryonic day 16 Wistar rats. Cells were extracted from the embryos and cultured with 1 μM MK801. Glial cell proliferation was stopped by adding 1 μM cytosine arabinoside after 3 h. Primary cultures of cortical neurons were transfected 96 h after plating using Lipofectamine 2000 reagent (Invitrogen) according to the manufacturer's instructions.

**Western blot and filter retardation assay**
Cells were harvested in PBS, pelleted, and lysed 30 min on ice in lysis buffer containing 50 mM Tris, pH 8.8, 100 mM NaCl, 5 mM $MgCl_2$, 0.5% NP-40, 1 mM EDTA, and 250 IU/ml benzonase (Merck) supplemented with a cocktail of protease inhibitors (Complete and Pefabloc; Roche). Total extracts were centrifuged at 13,000 rpm for 10 min at 4°C to separate soluble proteins from aggregates and membranes. Supernatants (30 μg protein) were analyzed by Western blot. Pellets were washed with PBS and further incubated 30 min on ice in a pellet buffer containing 20 mM Tris, pH 8.0, 15 mM $MgCl_2$, and 250 IU/ml benzonase. Protein concentrations (supernatant and pellet) were determined by Bradford assay (Bio-Rad Laboratories). Samples were prepared for Western blot and for filter assay as previously described (Sittler et al., 1998; Wanker et al., 1999).

**Pulse-chase analysis of ATXN7 turnover**
Pulse-chase experiments were performed 17 h after transfection of COS-7 cells with FL-74Q or with FL-74Q and PML IV. Cells were starved in methionine/cysteine-free DME containing 2% FBS for 1 h. Cells were labeled for 1 h with 200 μCi/ml of Pro-mix L-$^{35}$S labeling mix (GE Healthcare) in starvation medium. After the pulse, cells were rinsed twice and chased for the indicated periods of time in DME with 5% FBS. For immunoprecipitation, cells were lysed in 50 mM Tris, pH 8.0, 300 mM NaCl, 1% NP-40, 5% glycerol, and protease inhibitors. Equal amounts of labeled lysates ($12 \times 10^6$ cpm at time 0, determined after TCA precipitation) were immunoprecipitated with 3 μg anti-HA antibody (coupled to protein G–Sepharose beads) for 2 h at 4°C. Beads were washed four times with RIPA buffer, and bound proteins were directly denatured in 40 μl Laemmli buffer. Immunoprecipitates were resolved on 4–12% SDS gradient gels (Invitrogen), visualized by phosphoimaging, and quantified with Aida analysis software (Raytest GmbH).

**Immunofluorescence**
Cells plated on glass coverslips coated with poly-lysine (COS-7) or polyethyleneimine (cortical neurons) were fixed for 20 min with 4% paraformaldehyde. Primary neurons were fixed at 4 d after transfection. Permeabilization and further incubations with antibodies were done as previously described (Sittler et al., 1998). Cells were mounted with Fluoromount-G, and samples were observed with a confocal microscope (SP1; Leica) equipped with a 63×/1.32 NA objective. Leica confocal software was used to acquire images. For conventional analysis, we used a microscope (Axioplan-2; Carl Zeiss MicroImaging, Inc.) equipped with 25×/0.80 NA, 63×/1.40 NA, and 100×/1.40 NA objectives and a cooled mono 12-bits camera (Evolution QEi; Explora Nova). Fluo'Up software (Explora Nova) was used for image acquisition. 9-μm cryostat sections of fixed retina were prepared and used for immunofluorescence detection as described previously (Yvert et al., 2000).

**Antibodies**
For Western blot and immunofluorescence analysis, we used the following antibodies and concentrations: 1C1 mouse anti-ATXN7 (Yvert et al., 2000) at 1:5,000 (Western blot) and 1:1,000 (immunofluorescence), mouse anti-HA (Babco) at 1:10,000 (Western blot) and 1:4,000 (immunofluorescence), rabbit anti-ATXN7 (Affinity BioReagents, Inc.) at 1:500 (immunofluorescence), rabbit anti-ATXN7 affinity-purified polyclonal antibody 1261 at 1:100 (immunofluorescence on fixed retina only), mouse anti-PML (PG-M3; Santa Cruz Biotechnology, Inc.) at 1:500 (Western blot and immunofluorescence), rabbit anti-PML (H-238; Santa Cruz Biotechnology, Inc.) at 1:500 (Western blot and immunofluorescence), chicken anti-PML antibody at 1:500 (immunofluorescence on fixed retina only; a gift from H. de Thé, Centre National de la Recherche Scientifique, Paris, France), 1C2 anti-polyQ monoclonal antibody at 1:2,000 (Western blot), anti-FMRP 1C3 antibody (Sittler et al., 1996) at 1:1,000 (Western blot), mouse anti-polyubiquitinylated proteins (FK2; BIOMOL Research Laboratories, Inc.) at 1:1,000 (immunofluorescence), rabbit anti-19S proteasome subunit S10a (PW-8225; BIOMOL Research Laboratories, Inc.) at 1:500 (immunofluorescence), rabbit anti-20S core (PW-8155; BIOMOL Research Laboratories, Inc.) at 1:1,000 (immunofluorescence), rabbit anti-Hsp40 (SPA-400; StressGen Biotechnologies) at 1:2,000 (immunofluorescence). For the filter assay, we used the same antibody concentrations as for Western blots. For immunofluorescence, secondary antibodies were as follows: Alexa 488–conjugated goat anti–mouse or goat anti–rabbit IgG (Invitrogen) used at 1:500 and CY3-conjugated goat anti–mouse or goat anti–rabbit IgG (Jackson ImmunoResearch Laboratories) used at 1:1,000. In Fig. 1, different secondary antibodies and dilutions were used: CY3-conjugated goat anti–rabbit IgG (1:200) and FITC-conjugated goat anti–chicken IgG (1:150).

**Time-lapse recordings**
HeLa Kyoto cells (a gift from S. Narumiya, Kyoto University, Kyoto, Japan) grown on 35-mm microwell dishes (MatTek Corporation) were transfected with 1 μg FL-100Q-EGFP (expressing GFP-ATXN7 fusion protein) and 0.5 μg HcRFP-PML IV using FuGENE6 (Roche). At 6 h after transfection, cells were placed on the microscope in a chamber at 37°C and 5% $CO_2$. Several cells showing low levels of GFP-ATXN7 were selected and monitored every 10 min for 16 h. Images were acquired with an inverted microscope (DMIRE2; Leica) equipped with a 63×/1.35 NA objective and a camera (CoolSNAP fx; Roper Scientific). MetaMorph software (Molecular Devices) was used to control image acquisition and manipulation.

**Coimmunoprecipitation**
COS-7 cells were transfected in 90-mm culture dishes with PML IV and FL-74Q or -10Q. Cells were harvested 42–45 h after transfection and lysed on ice in 150 mM salt buffer (50 mM Tris, pH 8.0, 150 mM NaCl, 1 mM EDTA, and 1% NP-40) supplemented with a cocktail of protease inhibitors (Complete and Pefabloc). Total extract was centrifuged at 13,000 rpm for 10 min at 4°C, and the supernatant was precleared with protein A– or protein G–Sepharose beads (GE Healthcare) for 1 h at 4°C. Precleared supernatant and protein A– or protein G–Sepharose beads coupled with the appropriate antibodies were incubated 2 h at 4°C on a rotating wheel for immunoprecipitation. Finally, the beads were washed five times with 500 mM salt buffer (50 mM Tris, pH 8.0, 500 mM NaCl, 1 mM EDTA, and 1% NP-40; supplemented with protease inhibitors), and bound proteins were directly denatured by heating for 5 min at 95°C in 30 μl Laemmli buffer. Samples were analyzed by Western blot.

**Electron microscopy**
Cells were fixed with 4% paraformaldehyde in phosphate buffer, pH 7.4, for 1 h on ice and then postfixed with 1% osmium tetroxyde and embedded in Epon 812 (Taab). Ultrathin sections (50 nm) placed on nickel grids were immunogold labeled after embedding. We used primary antibodies mouse monoclonal anti–ATXN7 1C1 at 1:200 and rabbit polyclonal anti-PML at 1:250 and secondary antibodies conjugated to 10- or 15-nm gold particles (goat anti–mouse or goat anti–rabbit [Aurion]) at 1:100. After labeling, sections were postfixed in 1% glutaraldehyde and stained with uranyl acetate and lead citrate (see detailed protocol in the supplemental text). Cells were examined with an electron microscope (1200EX; Jeol) at 80 kV.

**Online supplemental material**
Fig. S1 shows that PML IV bodies recruit 19S5a, 19S6b, and 20Sα2 proteasome subunits. As a consequence, the colocalization of these actors of the protein degradation pathway with mutant ATXN7 strongly increases in double-transfected cells compared with cells expressing mutant ATXN7 alone. Online supplemental material is available at http://www.jcb.org/cgi/content/full/jcb.200511045/DC1.

Our thanks are due to A. Dejean, P. Kastner, and H. de Thé for the kind gifts of PML vectors, antibodies, and fruitful discussions; the confocal microscopy platforms of IFR 83 and 70, Paris; the imaging platform of Institut de Génétique et de Biologie Moléculaire et Cellulaire, Illkirch, for video microscopy; G. Yvert for mouse retina analysis; and J. Takahashi, G. Stevanin, H. El Hachimi, and J. Adamczewski for discussions.

A. Janer and M. Latouche are the recipients of fellowships from the French Ministry for Research. This work was financially supported by the VERUM Foundation and by grant LSHM-CT-2004-503304 from the European Union (to the EUROSCA consortium).

Submitted: 14 November 2005
Accepted: 30 May 2006

## References

Beech, S.J., K.J. Lethbridge, N. Killick, N. McGlincy, and K.N. Leppard. 2005. Isoforms of the promyelocytic leukemia protein differ in their effects on ND10 organization. *Exp. Cell Res.* 307:109–117.

Bischof, O., O. Kirsh, M. Pearson, K. Itahana, P.G. Pelicci, and A. Dejean. 2002. Deconstructing PML-induced premature senescence. *EMBO J.* 21:3358–3369.

Borden, K.L. 2002. Pondering the promyelocytic leukemia protein (PML) puzzle: possible functions for PML nuclear bodies. *Mol. Cell. Biol.* 22:5259–5269.

Cancel, G., C. Duyckaerts, M. Holmberg, C. Zander, G. Yvert, A.S. Lebre, M. Ruberg, B. Faucheux, Y. Agid, E. Hirsch, and A. Brice. 2000. Distribution of ataxin-7 in normal human brain and retina. *Brain.* 123:2519–2530.

Chai, Y., S.L. Koppenhafer, S.J. Shoesmith, M.K. Perez, and H.L. Paulson. 1999. Evidence for proteasome involvement in polyglutamine disease: localization to nuclear inclusions in SCA3/MJD and suppression of polyglutamine aggregation in vitro. *Hum. Mol. Genet.* 8:673–682.

David, G., N. Abbas, G. Stevanin, A. Durr, G. Yvert, G. Cancel, C. Weber, G. Imbert, F. Saudou, E. Antoniou, et al. 1997. Cloning of the SCA7 gene reveals a highly unstable CAG repeat expansion. *Nat. Genet.* 17:65–70.

Fogal, V., M. Gostissa, P. Sandy, P. Zacchi, T. Sternsdorf, K. Jensen, P.P. Pandolfi, H. Will, C. Schneider, and G. Del Sal. 2000. Regulation of p53 activity in nuclear bodies by a specific PML isoform. *EMBO J.* 19:6185–6195.

Goti, D., S.M. Katzen, J. Mez, N. Kurtis, J. Kiluk, L. Ben-Haiem, N.A. Jenkins, N.G. Copeland, A. Kakizuka, A.H. Sharp, et al. 2004. A mutant ataxin-3 putative-cleavage fragment in brains of Machado-Joseph disease patients and transgenic mice is cytotoxic above a critical concentration. *J. Neurosci.* 24:10266–10279.

Grignani, F., U. Testa, D. Rogaia, P.F. Ferrucci, P. Samoggia, A. Pinto, D. Aldinucci, V. Gelmetti, M. Fagioli, M. Alcalay, et al. 1996. Effects on differentiation by the promyelocytic leukemia PML/RARalpha protein depend on the fusion of the PML protein dimerization and RARalpha DNA binding domains. *EMBO J.* 15:4949–4958.

Grune, T., T. Jung, K. Merker, and K.J. Davies. 2004. Decreased proteolysis caused by protein aggregates, inclusion bodies, plaques, lipofuscin, ceroid, and 'aggresomes' during oxidative stress, aging, and disease. *Int. J. Biochem. Cell Biol.* 36:2519–2530.

Helmlinger, D., G. Abou-Sleymane, G. Yvert, S. Rousseau, C. Weber, Y. Trottier, J.L. Mandel, and D. Devys. 2004a. Disease progression despite early loss of polyglutamine protein expression in SCA7 mouse model. *J. Neurosci.* 24:1881–1887.

Helmlinger, D., S. Hardy, S. Sasorith, F. Klein, F. Robert, C. Weber, L. Miguet, N. Potier, A. Van-Dorsselaer, J.M. Wurtz, et al. 2004b. Ataxin-7 is a subunit of GCN5 histone acetyltransferase-containing complexes. *Hum. Mol. Genet.* 13:1257–1265.

Helmlinger, D., S. Hardy, G. Abou-Sleymane, A. Eberlin, A.B. Bowman, A. Gansmuller, S. Picaud, H.Y. Zoghbi, Y. Trottier, L. Tora, and D. Devys. 2006. Glutamine-expanded ataxin-7 alters TFTC/STAGA recruitment and chromatin structure leading to photoreceptor dysfunction. *PLoS Biol.* 4:e67.

Javed, A., and A.T. Reder. 2006. Therapeutic role of beta-interferons in multiple sclerosis. *Pharmacol. Ther.* 110:35–56.

Jensen, K., C. Shiels, and P.S. Freemont. 2001. PML protein isoforms and the RBCC/TRIM motif. *Oncogene.* 20:7223–7233.

Kastner, P., A. Perez, Y. Lutz, C. Rochette-Egly, M.P. Gaub, B. Durand, M. Lanotte, R. Berger, and P. Chambon. 1992. Structure, localization and transcriptional properties of two classes of retinoic acid receptor alpha fusion proteins in acute promyelocytic leukemia (APL): structural similarities with a new family of oncoproteins. *EMBO J.* 11:629–642.

Kaytor, M.D., L.A. Duvick, P.J. Skinner, M.D. Koob, L.P. Ranum, and H.T. Orr. 1999. Nuclear localization of the spinocerebellar ataxia type 7 protein, ataxin-7. *Hum. Mol. Genet.* 8:1657–1664.

Kruse, M.L., A. Arlt, A. Sieke, F. Grohmann, M. Grossmann, J. Minkenberg, U.R. Folsch, and H. Schafer. 2005. Immediate early gene X1 (IEX-1) is organized in subnuclear structures and partially co-localizes with promyelocytic leukemia protein in HeLa cells. *J. Biol. Chem.* 280:24849–24856.

La Spada, A.R., Y.H. Fu, B.L. Sopher, R.T. Libby, X. Wang, L.Y. Li, D.D. Einum, J. Huang, D.E. Possin, A.C. Smith, et al. 2001. Polyglutamine-expanded ataxin-7 antagonizes CRX function and induces cone-rod dystrophy in a mouse model of SCA7. *Neuron.* 31:913–927.

Lafarga, M., M.T. Berciano, E. Pena, I. Mayo, J.G. Castano, D. Bohmann, J.P. Rodrigues, J.P. Tavanez, and M. Carmo-Fonseca. 2002. Clastosome: a subtype of nuclear body enriched in 19S and 20S proteasomes, ubiquitin, and protein substrates of proteasome. *Mol. Biol. Cell.* 13:2771–2782.

McMahon, S.J., M.G. Pray-Grant, D. Schieltz, J.R. Yates III, and P.A. Grant. 2005. Polyglutamine-expanded spinocerebellar ataxia-7 protein disrupts normal SAGA and SLIK histone acetyltransferase activity. *Proc. Natl. Acad. Sci. USA.* 102:8478–8482.

Michalik, A., and C. Van Broeckhoven. 2003. Pathogenesis of polyglutamine disorders: aggregation revisited. *Hum. Mol. Genet.* 12:R173–R186.

Muratani, M., D. Gerlich, S.M. Janicki, M. Gebhard, R. Eils, and D.L. Spector. 2002. Metabolic-energy-dependent movement of PML bodies within the mammalian cell nucleus. *Nat. Cell Biol.* 4:106–110.

Nefkens, I., D.G. Negorev, A.M. Ishov, J.S. Michaelson, E.T. Yeh, R.M. Tanguay, W.E. Muller, and G.G. Maul. 2003. Heat shock and Cd2+ exposure regulate PML and Daxx release from ND10 by independent mechanisms that modify the induction of heat-shock proteins 70 and 25 differently. *J. Cell Sci.* 116:513–524.

Negorev, D., and G.G. Maul. 2001. Cellular proteins localized at and interacting within ND10/PML nuclear bodies/PODs suggest functions of a nuclear depot. *Oncogene.* 20:7234–7242.

Palhan, V.B., S. Chen, G.H. Peng, A. Tjernberg, A.M. Gamper, Y. Fan, B.T. Chait, A.R. La Spada, and R.G. Roeder. 2005. Polyglutamine-expanded ataxin-7 inhibits STAGA histone acetyltransferase activity to produce retinal degeneration. *Proc. Natl. Acad. Sci. USA.* 102:8472–8477.

Proctor, C.J., C. Soti, R.J. Boys, C.S. Gillespie, D.P. Shanley, D.J. Wilkinson, and T.B. Kirkwood. 2005. Modelling the actions of chaperones and their role in ageing. *Mech. Ageing Dev.* 126:119–131.

Qin, Q., R. Inatome, A. Hotta, M. Kojima, H. Yamamura, H. Hirai, T. Yoshizawa, H. Tanaka, K. Fukami, and S. Yanagi. 2006. A novel GTPase, CRAG, mediates promyelocytic leukemia protein-associated nuclear body formation and degradation of expanded polyglutamine protein. *J. Cell Biol.* 172:497–504.

Regad, T., and M.K. Chelbi-Alix. 2001. Role and fate of PML nuclear bodies in response to interferon and viral infections. *Oncogene.* 20:7274–7286.

Rockel, T.D., D. Stuhlmann, and A. von Mikecz. 2005. Proteasomes degrade proteins in focal subdomains of the human cell nucleus. *J. Cell Sci.* 118:5231–5242.

Sanchez, I., C. Mahlke, and J. Yuan. 2003. Pivotal role of oligomerization in expanded polyglutamine neurodegenerative disorders. *Nature.* 421:373–379.

Scheel, H., S. Tomiuk, and K. Hofmann. 2003. Elucidation of ataxin-3 and ataxin-7 function by integrative bioinformatics. *Hum. Mol. Genet.* 12:2845–2852.

Seeler, J.S., and A. Dejean. 1999. The PML nuclear bodies: actors or extras? *Curr. Opin. Genet. Dev.* 9:362–367.

Sittler, A., D. Devys, C. Weber, and J.L. Mandel. 1996. Alternative splicing of exon 14 determines nuclear or cytoplasmic localisation of fmr1 protein isoforms. *Hum. Mol. Genet.* 5:95–102.

Sittler, A., S. Walter, N. Wedemeyer, R. Hasenbank, E. Scherzinger, H. Eickhoff, G.P. Bates, H. Lehrach, and E.E. Wanker. 1998. SH3GL3 associates with the Huntingtin exon 1 protein and promotes the formation of polygln-containing protein aggregates. *Mol. Cell.* 2:427–436.

Skinner, P.J., B.T. Koshy, C.J. Cummings, I.A. Klement, K. Helin, A. Servadio, H.Y. Zoghbi, and H.T. Orr. 1997. Ataxin-1 with an expanded glutamine tract alters nuclear matrix-associated structures. *Nature.* 389:971–974.

Stevanin, G., A. Durr, and A. Brice. 2002. Spinocerebellar ataxias caused by polyglutamine expansions. *Adv. Exp. Med. Biol.* 516:47–77.

Takahashi, J., H. Fujigasaki, C. Zander, K.H. El Hachimi, G. Stevanin, A. Durr, A.S. Lebre, G. Yvert, Y. Trottier, H. The, et al. 2002. Two populations of neuronal intranuclear inclusions in SCA7 differ in size and promyelocytic leukaemia protein content. *Brain.* 125:1534–1543.

Takahashi, J., H. Fujigasaki, K. Iwabuchi, A.C. Bruni, T. Uchihara, K.H. El Hachimi, G. Stevanin, A. Durr, A.S. Lebre, Y. Trottier, et al. 2003. PML nuclear bodies and neuronal intranuclear inclusion in polyglutamine diseases. *Neurobiol. Dis.* 13:230–237.

Tanaka, M., Y. Machida, S. Niu, T. Ikeda, N.R. Jana, H. Doi, M. Kurosawa, M. Nekooki, and N. Nukina. 2004. Trehalose alleviates polyglutamine-mediated pathology in a mouse model of Huntington disease. *Nat. Med.* 10:148–154.

Wanker, E.E., E. Scherzinger, V. Heiser, A. Sittler, H. Eickhoff, and H. Lehrach. 1999. Membrane filter assay for detection of amyloid-like polyglutamine-containing protein aggregates. *Methods Enzymol.* 309:375–386.

Watase, K., E.J. Weeber, B. Xu, B. Antalffy, L. Yuva-Paylor, K. Hashimoto, M. Kano, R. Atkinson, Y. Sun, D.L. Armstrong, et al. 2002. A long CAG repeat in the mouse Sca1 locus replicates SCA1 features and reveals the impact of protein solubility on selective neurodegeneration. *Neuron.* 34:905–919.

Waza, M., H. Adachi, M. Katsuno, M. Minamiyama, C. Sang, F. Tanaka, A. Inukai, M. Doyu, and G. Sobue. 2005. 17-AAG, an Hsp90 inhibitor, ameliorates polyglutamine-mediated motor neuron degeneration. *Nat. Med.* 11:1088–1095.

Yoo, S.Y., M.E. Pennesi, E.J. Weeber, B. Xu, R. Atkinson, S. Chen, D.L. Armstrong, S.M. Wu, J.D. Sweatt, and H.Y. Zoghbi. 2003. SCA7 knockin mice model human SCA7 and reveal gradual accumulation of mutant ataxin-7 in neurons and abnormalities in short-term plasticity. *Neuron.* 37:383–401.

Yvert, G., K.S. Lindenberg, S. Picaud, G.B. Landwehrmeyer, J.A. Sahel, and J.L. Mandel. 2000. Expanded polyglutamines induce neurodegeneration and trans-neuronal alterations in cerebellum and retina of SCA7 transgenic mice. *Hum. Mol. Genet.* 9:2491–2506.

Yvert, G., K.S. Lindenberg, D. Devys, D. Helmlinger, G.B. Landwehrmeyer, and J.L. Mandel. 2001. SCA7 mouse models show selective stabilization of mutant ataxin-7 and similar cellular responses in different neuronal cell types. *Hum. Mol. Genet.* 10:1679–1692.

Zander, C., J. Takahashi, K.H. El Hachimi, H. Fujigasaki, V. Albanese, A.S. Lebre, G. Stevanin, C. Duyckaerts, and A. Brice. 2001. Similarities between spinocerebellar ataxia type 7 (SCA7) cell models and human brain: proteins recruited in inclusions and activation of caspase-3. *Hum. Mol. Genet.* 10:2569–2579.

Zhong, S., P. Salomoni, and P.P. Pandolfi. 2000. The transcriptional role of PML and the nuclear body. *Nat. Cell Biol.* 2:E85–E90.